Journal of controlled release

A neutral lipid envelope-type nanoparticle composed of a pH-activated and vitamin E-scaffold lipid-like material as a platform for a gene carrier targeting renal cell carcinoma

Hidetaka Akita[1,3,*], Ryohei Ishiba[1,3], Ryohei Togashi[1,3], Kota Tange[2], Yuta Nakai[2], Hiroto Hatakeyama[1], Hideyoshi Harashima[1,]**

***** Corresponding author. Tel.: +81 11 706 3735; fax: +81 11 706 4879

****** Corresponding author. Tel.: +81 11 706 3919; fax: +81 11 706 4879

[1]Laboratory for Molecular Design of Pharmaceutics, Faculty of Pharmaceutical Science, Hokkaido University, Kita-12, Nishi-6, Kita-ku, Sapporo, Japan

[2]NOF Corporation, 3-3 Chidori-cho, Kawasaki-ku, Kawasaki, Kanagawa 210-0865, Japan

[3] These authors equally contributed to this study. The authors are listed alphabetically in accordance with family name.

E-mail addresses: akita@pharm.hokudai.ac.jp (H. Akita), harashima@pharm.hokudai.ac.jp (H. Harashima)

Keywords: cancer, gene delivery, renal carcinoma, angiogenesis

Abstract

A renal cell carcinoma (RCC) is one of the refractory tumors, since it readily acquires resistance against chemotherapy. Thus, alternative therapeutic approaches such as obstructing the neovasculature are needed. We previously reported on the development of a plasmid DNA (pDNA)-encapsulating liposomal nanoparticle (LNP) as a hepatic gene delivery system that is applicable to systemic administration. The key molecular component is a SS-cleavable and pH-activated lipid-like material (ssPalm) that mounts dual sensing motifs (ternary amines and disulfide bonding) that are responsive to the intracellular environment. The main purpose of the present study was to expand its application to a tumor-targeting gene delivery system in mice bearing tumors established from a RCC (OS-RC-2). When the modification of the surface of the particle is optimized for the polyethyleneglycol (PEG), stability in the blood circulation is improved, and consequently tumor-selective gene expression can be achieved. Furthermore, gene expression in the tumor was increased slightly when the hydrophobic scaffold of the ssPalm was replaced from the conventionally used myristic acid (ssPalmM) to α-tocopherol succinate (ssPalmE). Moreover, tumor growth was significantly suppressed when the completely CpG-free pDNA encoding the solute form of VEGFR (fms-like tyrosine kinase-1: sFlt-1) was used, especially when it was delivered by the LNP formed with ssPalmE ($LNP_{ssPalmE}$). Thus, the PEG-modified $LNP_{ssPalmE}$ is a promising gene carrier for the cancer gene therapy of RCC.

Keywords: cancer, gene delivery, renal carcinoma, angiogenesis

1. Introduction

Gene therapy has been proposed as a new-generation strategy for curing intractable diseases as well as genetic disorders that have plagued civilization [1]. While the gene therapy approach has faced technical and/or regulatory impediments, a large number of clinical trials are still ongoing worldwide. One crucial success is the first approval of the Glybera® (UniQure) by the European Medicinal Agency (EMA) as a first gene-based medication outside China that accompanies a substantial impact from the regulatory perspective point of view [2, 3]. While success is now

limited to ultra-orphan condition (a prevalence of <0.1 per 10000 persons in the European Union), this historical achievement promises to reinforce the scientific community to realize the significance of the gene therapy.

The prevalence rate of renal cell carcinoma (RCC) has been growing worldwide, especially in advanced nations in the past decades [4-7], while RCC is now considered to be an orphan situation (a prevalence of approx. 3 per 10000 persons in European Union) [3]. One of the serious problems associated with RCC is that it readily acquires resistance to a wide variety of drugs [7, 8] by the up-regulation of multi-drug export pumps such as the p-glycoprotein[9]. Thus, alternative strategies such as immunotherapy [10, 11] or anti-angiogenic therapy using molecular-targeting agents against vascular endothelial growth factor (VEGF) and the mammalian target of rapamycin (mTOR) [12] are currently a challenge. However, the systemic administration of the VEGF inhibitor (i.e. bevacizumab) is accompanied by risks for developing adverse effects such as hypertension [13]. Thus, the tumor specific expression of anti-angiogenic factors by means of transgene delivery can be considered to be a rational strategy.

While the share of the viral approach in total clinical trials of gene therapy remains high (>65%), the value of non-viral approaches is on the rise [14]. Since the first report of the successful transfection of plasmid DNA (pDNA) using a cationic lipoplex [15], the compaction of the pDNA with cationic materials (polycations or liposomes) had been a common strategy, based on the assumption that the cationic charge is a key driving force for cellular association, aided by the negatively charged heparan sulfate on the cell surface [16]. However, for effective transgene expression by non-viral approaches, further improvement of the carriers are prerequisite in terms of controlling intracellular trafficking (i.e. endosomal escape and nuclear transport) and, to maximize the post-nuclear delivery processes (i.e. transcription and translation). In particular, quantitative analysis of the intracellular disposition of the pDNA transfected by cationic carriers (i.e. polycations [17] or a lipoplex [18, 19]) in comparison with that of adenovirus has demonstrated that post-nuclear processes are crucial rate-limiting processes in cationic carriers when transfected to dividing cells. Further analysis revealed that electrostatic interactions of the cationic component with the pDNA cargo or mRNA are the cause of the poor transcription and translation efficacy [18, 19]. For the challenge in systemic applications for the tumor targeting, pharmacokinetic aspects (stability in the blood circulation and tissue selectivity)

and safety must also be taken into the consideration. The risk associated with the systemic administration of a cationic carrier is the formation of aggregates with erythrocytes [20, 21] and/or platelets [22], and the resulting obstructions in lung capillaries.

One of the rational strategies for overcoming the above mentioned drawback is to develop a pDNA-encapsulated particle that is neutral in the physiological environment of the blood circulation, extracellular domains and the cytoplasm. On the other hand, the presence of a cationic charge is a crucial driving force for endosomal escape. Thus, a pH-sensitive lipid that can develop a positive charge in response to the low pH-environment in endosomes is a reasonable molecular design. The pioneering technology involved the production of stabilized plasmid-lipid particles (SPLP) [23-25] or pre-condensed stable plasmid lipid particles (pSPLP) [26] that are formed using ionizable lipids with ternary amine structures. More recently, a liposomal nanoparticle (LNP) formed using various types of ionizable lipids has been developed for use as a siRNA carrier targeting the liver [27-29] or tumors [30, 31]. As an alternative molecular platform, in a previous study, we reported on the development of a SS-cleavable Proton-Activated Lipid-like Material (ssPalm) [32]. The unique design of this material is that it mounts dual sensing motifs that can respond to various intracellular environments; tertiary amines as a proton sponge unit responsible for an acidic compartment (endosome/lysosome) for membrane destabilization, and disulfide bonding that can be cleaved in a reducing environment (the cytosol).Myristic acid was used as a 1st generation ssPalm as a hydrophobic scaffold (ssPalmM). The molecule allows the prepared liposomal nanoparticle ($LNP_{ssPalmM}$) to escape from endosomes, and subsequently to be collapsed in cytoplasm, thus permitting the efficient decapsulation of pDNA. As a result, the particle exhibited a high gene expression *in vitro* HT1080 cell culture comparable to that of cationic particles, with a small amount of cellular uptake and minimum cytotoxicity. Moreover, once the pDNA was encapsulated into the $LNP_{ssPalmM}$, the pDNA was resistant to enzymatic degradation in serum for at least 24 h [32]. In addition, the $LNP_{ssPalmM}$ flows into sinusoidal capillaries without aggregate formation, and thereby accumulating in hepatocytes within 10 min. As a result, hepatocyte-specific and long-lasting gene expression was achieved [33]. Thus, such a particle would be highly desired for use in gene delivery via *i.v.* administration.

In the present study, we attempted to expand its application to tumor-targeting gene delivery using the neutralized liposomal nanoparticles prepared using the 2nd generation of ssPalm, where fat-soluble vitamins were used as a hydrophobic scaffold. Very recently, we reported on the preparation of a vitamin A (retinoic acid)-scaffold ssPalm (ssPalmA) that can accelerate nuclear transfer in certain types of cells (i.e. HT1080) [34]. As an original material in the present study, we report on the use of ssPalmE, where vitamin E (α-tocopherol succinate) was employed as a hydrophobic scaffold. We identified an anti-tumor effect of RCC by the expression of the solute form of VEGFR (fms-like tyrosine kinase-1: sFlt-1) as an endogenous molecule, which can compete against the binding of VEGF to the VEGFR for anti-angiogenesis [35].

2. Materials and Methods

2.1. Materials

1-stearoyl-2-dioleoyl sn-glycero-3-phosphatidylethanolamine (SOPE) and Cholesterol were purchased from Avanti Polar Lipids (Alabaster, AL). 1-stearoyl-2-oleoyl-sn-glycero-3-phosphocholine (SOPC) was purchased from NOF Corporation (Tokyo, Japan). 1-(monomethoxy polyethyleneglycol2000)-2,3-dimstearylglycerol (PEG_{2000}-DSG) and 1-(monomethoxy polyethyleneglycol5000)-2,3-distearylglycerol (PEG_{5000}-DSG) was purchased from the NOF Corporation (Kanagawa, Japan). [cholesteryl-1,2-3 H(N)]-cholesteryl hexadecyl ether ([^{3}H]CHE) was purchased from PerkinElmer Co. Ltd. (Waltham, MA).

Male ICR mice (5-6 weeks old) were obtained from Japan SLC (Shizuoka, Japan). 4-week-old male BALB/cAJcl-*nu/nu* mice were purchased from CLEA Japan. The experimental protocols were reviewed and approved by the Hokkaido University Animal Care Committee in accordance with the "Guide for Care and Use of Laboratory Animals". In all experiments, the animals were used without fasting. The scheme for the chemical synthesis of the ssPalmM, ssPalmA and ssPalmE is shown in **Supplemental Information**.

2.2. Construction of pDNA

Conventional pDNA encoding luciferase (GL3) (pcDNA3.1-GL3) was constructed as described previously [36]. To prepare pDNA encoding luciferase that is completely free from unmethylated CpG dinucleotide motifs (pCpGfree-Luc(0)), the multiple cloning site of pCpGfree-mcs (Invivogen, San Diego, CA, USA) was preliminarily replaced with a new one that can be digested by 5'-Bgl II-Pvu II-Nco I-Sca I-Xba I-Nhe 1-3' by ligating the hybridized

oligonucleotide fragments to the Bgl II / Nhe I digestion of pCpGfree-mcs (pCpGfree-NEWmcs). Thereafter, a fragment encoding the CpG-free luciferase that accompanies the one CpG motif just below the stop codon; Luc(+1) was obtained by the Nco I/Nhe I digestion of pORF-Luc;;Sh-CpG (Invivogen), and ligated to the Nco I / Nhe I digested site of pCpGfree-NEWmcs (pCpGfree-Luc(+1)). Finally, the last remaining CpG motif was removed by inserting a CpG motif-free nucleotide fragment into a Dra III / Nhe I digested site of pCpGfree-Luc(+1), where we refer it a pCpGfree-Luc(0).

For the preparation of the completely CpG-free pDNA encoding mouse sFlt-1, CpG-free insert encoding sFlt-1, with GCCACC just above the start codon as a Kozak sequence was custom-synthesized (Life Technologies Japan. Ltd. Tokyo, Japan). In this synthesis, GATATCT sequences were also added at both of 5'-end (just above the Kozak sequence) and 3'-end (just below the stop codon) to allow these sequences to be cleaved by EcoRV. The open reading frame of the CpG-free mouse sFlt-1 is shown in **Supplemental Figure S1**. The insert encoding CpG-free sFlt-1 was obtained by the EcoRV digestion, and ligated to the PvuII digested site of pCpGfree-NEWmcs (pCpGfree-sFlt-1(0)). Both of pDNA was purified using a Qiagen Endofree plasmid Mega Kit (Qiagen GmbH, Hilden, Germany).

2.3. Preparation of liposomal nanoparticles encapsulating pDNA (LNP)

LNPs were prepared by the ethanol dilution method [32] of a larger scale for *in vivo* use. First, pDNA/protamine core particles were prepared at an acidic pH. pDNA and protamine solutions (0.3 mg/mL and 0.24 mg/mL) were prepared in 10 mM HEPES buffer (pH5.0-5.4). pDNA particles at a nitrogen/phosphate (N/P) ratio of 1.2 were prepared by the drop-wise addition of 350 μL of the protamine solution (0.24 mg/ml) into the 350 μl of the DNA solution (0.3 mg/ml) with vortexing. Second, pDNA/protamine core particles were encapsulated into the envelope formed with ssPalm and the helper lipids. The lipids composed of ssPalmX (X; M or A or E):helper lipid (SOPE or SOPC):Chol (3:4:3) plus 3 mol% of DMG-PEG_{2000} (1155 nmol in total lipids) were dissolved in 700 μL of ethanol. Under vortex mixing at room temperature, the lipid solution (700 μL) was rapidly diluted with an equal volume of the pDNA/protamine core particle suspension (50 vol% ethanol). The solution was further diluted with 6.3 mL of 10 mM HEPES (pH5.0-5.4) to 5 vol% ethanol. The diluted solution was concentrated by ultrafiltration using an Amicon Ultra 15 filter (Millipore Corp. Billerica, MA) by centrifugation at 1,000g for 15 min at

room temperature. The particle solution remaining on the upper column was diluted with 7 mL of 100 mM HEPES (pH=7.4), and again concentrated by centrifugation at 1,000g for 20 min at room temperature. Finally, the particles were diluted with 10 mM HEPES (pH=7.4) to achieve the desired concentration. In an attempt to enhance the stability in the blood circulation, the indicated amount of DSG-PEG_{2000} or DSG-PEG_{5000} (5mol% or 10 mol% of total lipid) stocked in 10mM HEPES (pH=7.4) was added to the prepared particle solution, and the resulting suspension was then further incubated at 60 ^{o}C for 30 min.

The diameter and ξ-potential of the LNP and core particles were determined using an electrophoretic light-scattering spectrophotometer (Zetasizer; Malvern Instruments Ltd., Malvern, WR, UK).

2.4. Pharmacokinetic analysis

To evaluate the time profile of blood concentration of LNPs, the particles were labeled with [^{3}H]CHE, as a lipid marker. The LNPs were intravenously administered via tail vein at a dose of 40 μg pDNA/mouse. At indicated times, the radioactivity in the blood was counted as described previously [37, 38].

2.5. Evaluation of the pDNA content and gene expression in tumor tissue

OS-RC-2 cells, established from a renal cell carcinoma were kindly gifted by Drs. Kyoko Hida and Noritaka Ohga (Graduate School of Dental Medicine, Hokkaido University). The cells were cultured in RPMI-1640 medium supplemented with 10% fetal bovine serum, penicillin (100 U/mL) and streptomycin (100 μg/mL). For preparing OS-RC-2-bearing mice, 1.0 x 10^{6} cells in 75 μL of sterilized PBS were inoculated into the anesthetized BALB/cAJcl-*nu/nu* mice in the right flask. Tumor volume was calculated by the following formula: (major axis × minor axis^{2}) ×0.52. When the tumors reached sizes of approximately 200 cm^{3} (approximately 15 days after tumor inoculation), LNPs corresponding to the 40 μg pDNA/mouse were intravenously injected.

For quantifying the amount of pDNA, a 100 mg sample of tumor section was placed in 1 mL of homogenate buffer (3 mM Tris-HCl, 0.1 mM ethylenediaminetetraacetic acid, 250 mM sucrose, pH 7.4), and was then homogenized with MAZELA (EYELA, Tokyo Japan). The homogenate was transferred to an Eppendorf tube, and then centrifuged at 3000 rpm for 10 min at 4^{o}C. The DNA was isolated from the pellet using a Sepa Gene kit (Sanko Jun-yaku, Tokyo, Japan) according to the manufacture's protocol. The DNA samples were incubated at 98^{o}C for 10 min,

and allowed to stand on ice until used. A 25 μl aliquot of the reaction mixture that included 5 μl of diluted DNA sample (1:500 in water), 5 pmol of a set of primers to amplify the luciferase gene fragment: 5'-GGAGCCTACAAGACTACAAGATCCAG-3' and 5'-GTCATACTTGTCAATGAGGGTGCTC-3', and 12.5 μl of 2x SYBR Green Master Mix (Toyobo, Osaka, Japan) was subject to PCR using the Agilent Stratagene QPCR System Mx3000P (Agilent, Foster City, CA, USA). The DNA was denaturized at 95 ^{o}C for 15 s, and annealed at 60 ^{o}C for 1 min and extended at 72 ^{o}C for 30 sec. The denaturation/annealing cycle was repeated 40 times. To evaluate the absolute number of pDNA copies, a series of diluted naked DNA was used to prepare a standard curve. The number of gene copies was normalized by the total DNA amount in the sample (μg).

At 48 h post-injection, the mice were sacrificed, and the tumor tissues were collected. Tumor tissues were homogenized in Reporter Lysis Buffer (1 ml), using a POLYTRON homogenizer (KINEMATICA), followed by centrifugation at 13000 rpm for 10 min at 4 °C and the supernatant was obtained. The luciferase activity in the supernatant (20 μl) was assayed using the Luciferase Assay System (Promega, Madison, WI). The relative light units (RLU) were measured using a luminometer (Bio-instrument ATTO Luminescencer AB-2200, JAPAN), and normalized to the protein content that were estimated using the bicinchoninic acid (BCA) protein assay (Bio-Rad).

For visualizing gene expression, LNPs composed of the ssPalmE/SOPC/Chol (3/4/3) plus 3mol% of DMG-PEG_{2000} and 5 mol% of DSG-PEG_{5000}, were injected into mice via the tail vein at a dose of 40 μg pDNA/mouse. At 6 h after administration, 200 μL VivoGlo™ Luciferin, *in vivo* grade (Promega) was injected at a dose of 3 mg/mouse into the peritoneal cavity 5 min prior to *in vivo* imaging with the IVIS Lumina II (Xenogen, Alameda, CA, USA). Images were obtained using a 1-min exposure time. During the measurement, the mice were anesthetized with isoflurane on a stage kept at 25 °C.

2.6. Anti-tumor effect

The OS-RC-2-bearing mice were prepared as described above. When the tumor were grown to approximately 70 mm^3 (approximately 10 days after the tumor inoculation), PBS, $LNP_{ssPalmM}$ and $LNP_{ssPalmE}$ encapsulating pCpGfree-sFlt-1(0) or pCpGfree-Luc(0) were administered

intravenously at a dose of 37.5 μg of pDNA/mouse 3 times at every 3 days. The growth of the tumor is represented as the tumor volume (mm^3).

2.7. mRNA expression of sFlt-1 and anti-angiogenic effect

OS-RC-2-bearing mice were prepared as described above. To evaluate the mRNA expression of sFlt-1 by RT-PCR, PBS, $LNP_{ssPalmE}$ encapsulating pCpGfree-sFlt-1(0) or pCpGfree-Luc(0) were administered intravenously at a dose of 37.5 μg pDNA/mouse. At 48 h after the administration, approximately 50 mg of tumor tissue was collected in screw cap tube with the TRIzol Reagent (Life Technologies, Carlsbad, CA) and 5 mm zirconia beads (ZB-50; Tomy, Tokyo, Japan) added and the resulting suspension was homogenized with a Micro Smash MS-100R (Tomy) at 4800 rpm for 30 sec at 4 ^{O}C, twice. The RNA was extracted from this homogenate according to the manufacture's protocol. 1 μg of total RNA in 4.5 μL in water was incubated at 65^{o}C for 5 min, and then allowed to stand on ice until used. The RNA was reverse transcribed using the high-capacity RNA-to-cDNA Kit (ABI, Foster City, CA), according to the manufacturer's instructions (42^{o}C for 60 min, and then at 95 ^{o}C for 5 min). For the PCR reaction to amplify the sFlt-1 or β-actin fragment, the cDNA was diluted with water 5- and 10-fold, respectively. 1 μL aliquot of the diluted cDNA was used in a 20 μl PCR reaction containing specific primer sets (4 pmol each), 0.4 μL of 4mL dNTP mix, Taq DNA Polymerase (New England Biolabs; Beverly, MA) and Standard 10x Taq Buffer (New England Biolabs; Beverly, MA). Primers for the experiment were as follows: sFlt-1 forward, 5'- TGGTGTACAGTAGCTTCCAAGG-3'; reverse, 5'-GCCTGTTATTCCTCCCACAGG-3'; β-actin forward, 5'-AGAGATGGCCACGGCTGCTT-3'; reverse, 5'- TACATGGTGGTGCCGCCAGA-3', and then were subjected to the PCR reaction by C1000 Touch Thermal Cycler (Bio-Rad, Hercules, CA, USA). The DNA was denaturized at 95 °C for 30 s, and annealed at 58 °C for 30 sec. Extension was performed at 68 °C for 10 sec. This process was repeated for 30 cycles. As a control, PCR was performed without reverse transcription. The amplification of the DNA fragments was analyzed by gel electrophoresis on 2% (w/v) agarose, followed by staining with Gelred (Biotium, Hayward, CA, USA).

For the evaluation of the anti-angiogenic effect, PBS, $LNP_{ssPalmE}$ encapsulating pCpGfree-sFlt-1(0) or pCpGfree-Luc(0) were administered intravenously at a dose of 37.5 μg pDNA/mouse twice at 3-day interval. At 2 day after the second administration, tumor tissues were collected

and placed in 4% formaldehyde for fixation at 4 ^{o}C overnight. The tissue was then incubated in 20% sucrose at 4 ^{o}C for 24 h. Thereafter, the sample was embedded in OCT compound (Tissue-Tek, Sakura Finetek, Torrance, Calif., USA) and quick-frozen in liquid nitrogen. The sections (10 μm thick) mounted on glass slides. The tissue sections were treated with a 50-fold dilution of FITC–GSI-B4 (FL-1201, Vector Laboratories, Burlingame, CA) for 30 min. Confocal images were obtained using a Nikon A1 microscope equipped with an objective lens (Plan Apo VC 20x DIC N2).

To quantify the FITC–GSI-B4-positive pixel counts, 10 randomly captured images per group were exported to the freely available software ImageJ version 1.48 (http://rsb.info.nih.gov/ij/index.html). The density of the tumor vasculature is represented as a fraction of the FITC–GSI-B4-positive pixel area to the total in one picture.

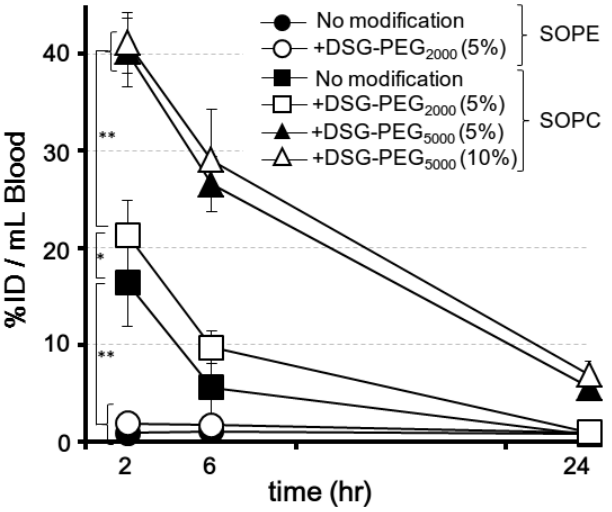

Fig.1. Time profiles for the concentration of $LNP_{ssPalmM}$ in the blood.

The $LNP_{ssPalmM}$ modified with DSG-PEG_{2000} or DSG-PEG_{5000} at various density (5% or 10%) were labeled with [^{3}H]CHE, and then administered intravenously. The time profiles for the blood concentration were represented by %ID/mL. Circle and square symbols represent the $LNP_{ssPalmM}$ prepared with SOPE and SOPC as a helper lipid, respectively. Open and closed symbols represent the $LNP_{ssPalmM}$ modified with DSG-PEG_{2000} and unmodified one, respectively. The triangles represent the $LNP_{ssPalmM}$ prepared with SOPC that were modified with 5mol% (closed symbols) and 10 mol% (open symbols) of DSG-PEG_{5000}, respectively. Data were represented as the mean ± S.D. of triplicate experiments. Statistical analyses were performed by One-way ANOVA followed by Bonferroni's multiple comparison test (*; $p<0.05$, **; $p<0.01$).

3. Results

3.1. Time profile for nanoparticles concentration in the blood circulation

In our previous report, we optimized the lipid composition of the $LNP_{ssPalmM}$ as ssPalmM/SOPE/Chol (3/4/3) to maximize the transgene expression in *in vitro* cultured HT1080 cells. To allow the neutral particles to remain dispersed, hydrophilic layers were formed on the surface of the particle by incorporating 3 mol% of DMG-PEG_{2000}. The main purpose of this study was to upgrade

this particle to the level of a tumor delivery system that would be applicable via intravenous administration. It is generally recognized that liposomal nanoparticles that are stable in blood gradually accumulate in tumor tissue through the leaky neovasculature by the enhanced permeability and retention (EPR) effect[39]. In an attempt to prolong the lifetime of particles in the blood circulation, the surface of the $LNP_{ssPalmM}$ were modified with DSG-PEG_{2000} in which longer carbohydrate chains (C_{18}) was used as a hydrophobic scaffold, as demonstrated previously [23] (**Figure 1**). The concentration of *in vitro* optimized particles became rapidly diminished to <2%ID/mL within at least 2 h after the administration (closed circle). Furthermore, even when the surface was modified with 5 mol% DSG-PEG_{2000}, the stability in the blood remained poor (open circle). Thus, the helper lipid was replaced with SOPC. As a result, the blood concentration increased even in the case of PEG-unmodified particles (closed square). In addition, the modification with DSG-PEG_{2000} significantly prolonged the lifetime of the particles in the blood circulation (open square). To further enhance this, the length of the PEG was extended by modification with DSG-PEG_{5000}, instead of DSG-PEG_{2000}. Consequently, the concentration of the particles in the blood increased drastically, by approximately 2 folds (closed triangle). Of note, additional modification with DSG-PEG_{5000} (10 mol%) did not result in any

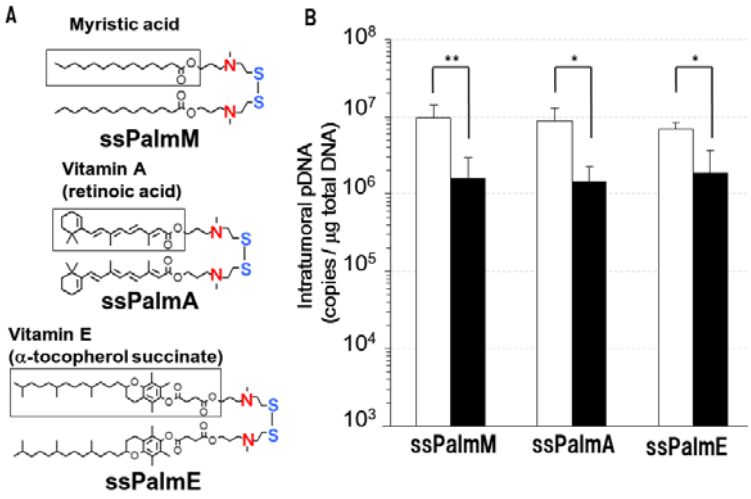

Fig.2. Effect of the hydrophobic scaffold on the accumulation and stability of pDNA in tumor tissue

(A) Chemical structures of ssPalmM, ssPalmA and ssPalmE. Myristic acid, retinoic acid and α-tocopherol succinate were used as a hydrophobic scaffold. These materials mount ternary amines as a proton-sponge unit and disulfide bonding as a reductive environment-responsive cleavage unit. (B) Tumor samples were collected at 24 h (closed bars) and 48 hr (open bars) after the intravenous administration of $LNP_{ssPalmM}$, $LNP_{ssPalmA}$ and $LNP_{ssPalmE}$ for the separation of total DNA. The DNA samples were subjected to real-time PCR for the quantification of copy numbers of pDNA in tumor. Data are expressed as the mean ± S.D. of triplicate experiments. Statistical analyses were performed by One-way ANOVA followed by Student-Newman-Keuls test (*; $p<0.05$, **; $p<0.01$).

further improvement in the blood circulation profile (open triangle). The sizes and ξ-potentials of the particles were listed in **Table 1**. All of the $LNP_{ssPalmM}$ were 100~150 nm in average, and neutral in ξ-potential. Thus, the difference in blood circulation profiles (**Figure 1**) cannot be explained from the point of view of the physicochemical characteristics of the preparations. In the following study, LNPs modified with 5 mol% of DSG-PEG_{5000} were used as the platform for the gene carrier targeting tumor tissues.

3.2. Effect of the hydrophobic scaffold on the accumulation and stability of LNP in tumor tissue

We investigated the effect of the hydrophobic scaffold on the *in vivo* accumulation and subsequent stability of pDNA in OS-RC-2 tumors. The chemical structures of the ssPalmM, ssPalmA and ssPalmE used in this study are shown in **Figure 2A**. In the ssPalmA and ssPalmE, retinoic acid and α-tocopherol succinate were employed, respectively, as a hydrophobic scaffold instead of myristic acid. The structure of the hydrophobic scaffold had no significant effect on the physicochemical characteristics of the particles, while the ξ-potential of $LNP_{ssPalmE}$ was slightly less than these for the others (approximately -6.5 mV) (**Table 1**).

At 24 or 48 h after the injection of LNPs prepared with ssPalmM, ssPalmA and ssPalmE, the pDNA was extracted from the OS-RC-2 tumors, and the number of gene copies of pDNA was then evaluated by quantitative PCR. As shown in **Figure 2B**, the amount of pDNA is nearly the same at both of 24 h and 48 h after the injection, regardless of the type of ssPalm used. Thus, the structure of the hydrophobic scaffold has only a minor effect on the pharmacokinetics of the LNPs and their stability after they reach the tumor tissue.

	Size (nm)	PDI	ξ-potential (mV)
ssPalm**M**/SOPE/Chol	153.0	0.21	- 2.2
ssPalm**M**/SOPC/Chol	119.8	0.19	-0.6
ssPalm**M**/SOPC/Chol +5mol% DSG-PEG_{2000}	143.0	0.26	+ 0.2
ssPalm**M**/SOPC/Chol +5mol% DSG-PEG_{5000}	133.7	0.18	- 0.9
ssPalm**M**/SOPC/Chol +10mol% DSG-PEG_{5000}	136.6	0.20	-1.7
ssPalm**A**/SOPC/Chol +5mol% DSG-PEG_{5000}	152.2	0.14	-4.7
ssPalm**A**/SOPC/Chol +10mol% DSG-PEG_{5000}	149.9	0.17	-2.2
ssPalm**E**/SOPC/Chol +5mol% DSG-PEG_{5000}	132.7	0.17	-6.7
ssPalm**E**/SOPC/Chol +10mol% DSG-PEG_{5000}	133.5	0.16	-6.5

Table 1. Physicochemical characters of LNPs

3.2. in vivo transgene expression in tumors and liver

The transgene expression of the marker gene (luciferase) in tumors, as well as the liver was evaluated at 48 h after injection (**Figure 3**), since we recently reported that an $LNP_{ssPalmM}$ composed of ssPalmM/SOPC/Chol modified with 3 mol% of DSG-PEG_{2000} showed liver-specific gene expression, and the gene expression in normal mice reached a plateau at 48h[33]. Hyde et al. previously reported that the complete deletion of the unmethylated CpG-motifs from the pDNA conferred sustained gene expression with minimal inflammatory response in the lung after an *in vivo* aerosol delivery of a cationic lipoplex [40]. Consistent with that observation, we also found that the $LNP_{ssPalmM}$ encapsulating pDNA that was free from the CpG motifs ((pCpGfree-Luc(0)) exhibited the higher gene expression in the liver in comparison with conventionally used pDNA (pcDNA3.1-GL3) [33]. Thus, in this study, we encapsulated pCpGfree-Luc(0) as a marker gene.

The findings confirmed that the transgene expression of the *in vitro* optimized $LNP_{ssPalmM}$ (SOPE as a helper lipid) was at nearly the background level in both tumor tissue and the liver. In contrast, a reliable reading of gene expression was observed both in tumors and the liver after the injection of $LNP_{ssPalmM}$ (SOPC as a helper lipid) modified with 5 mol% DSG-PEG_{2000}. Moreover, the gene expression in tumor tissue was increased when the preparation was modified with 5 mol% or 10 mol% DSG-PEG_{5000}, while hepatic gene expression decreased in a density-

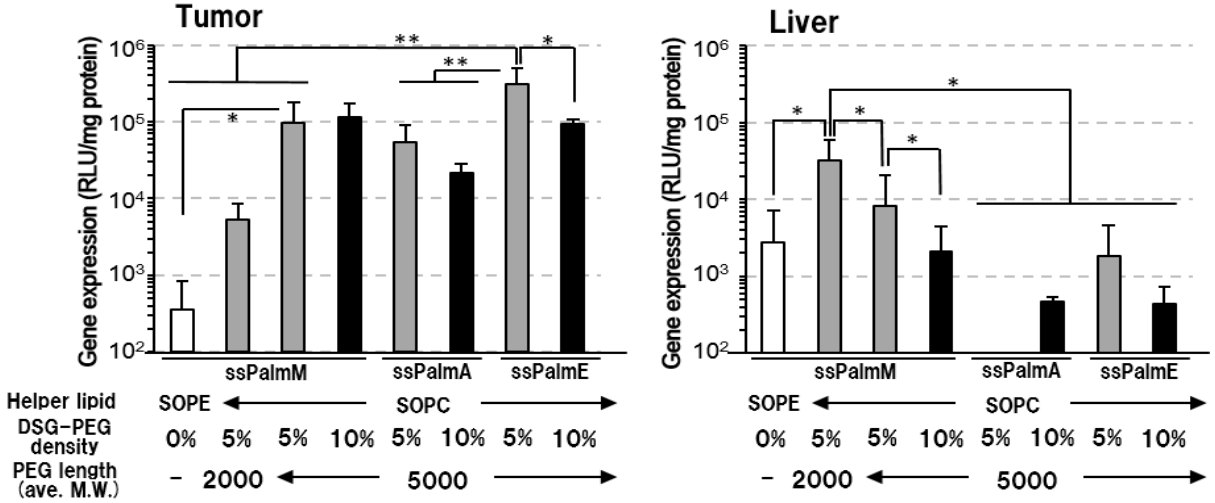

Fig.3 Effect of the hydrophobic scaffold on the accumulation and stability of pDNA in tumor tissue

LNP was prepared using various combinations of ssPalms (ssPalmM, ssPalmA and ssPalmE), helper lipids (SOPE and SOPC) and PEG lipids (DSG-PEG_{2000} and DSG-PEG_{5000}). Transfection activities were evaluated at 48 h after the intravenous administration of the particles at a dose of 40 μg/mouse. Statistical analyses were performed by One-way ANOVA followed by Newman-Keuls multiple comparison test (*; $p<0.05$, **; $p<0.01$).

dependent manner. These data are consistent with the general concept that the efficacy of spontaneous tumor accumulation via the EPR effect is correlated with the stability of the particle in the blood circulation (**Figure 1**).

Transgene expression of $LNP_{ssPalmA}$ or $LNP_{ssPalmE}$ modified with DSG-PEG_{5000} was then compared with that of the $LNP_{ssPalmM}$. As a result, a significantly higher gene expression was achieved in the case of the $LNP_{ssPalmE}$ when it was modified with 5 mol% DSG-PEG_{5000}. It is noteworthy that the hepatic gene expression of $LNP_{ssPalmA}$ or $LNP_{ssPalmE}$ was decreased to the background level. The tumor-specific gene expression was also confirmed by the *in vivo* imaging of the luciferase activity (**Figure 4**). It is noteworthy that gene expression was not detectable at 6 h after injection, but was increased in a time dependent manner up to 24 h. Gene expression reached plateau within 48, and was detectable at least until 72 h. Changes in the lipid composition of the ssPalmE/SOPC/Chol to 5/2/3 or 1/6/3 resulted in a decreased tumor gene expression (data not shown). Collectively, it can be concluded that an $LNP_{ssPalmE}$ composed of ssPalmM/SOPC/Chol (3/4/3) modified with 5 mol% of DSG-PEG_{5000} is an *in vivo* optimized particle for achieving tumor specific gene delivery.

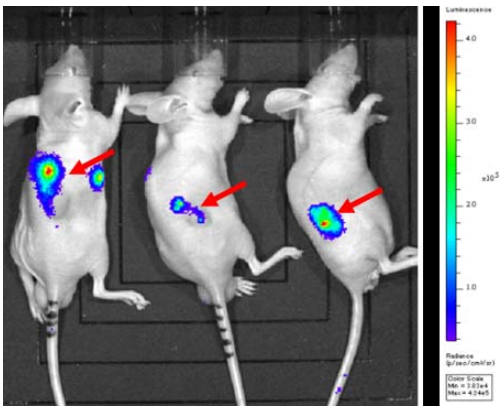

Fig.4 Optical images of the in vivo transgene expression

Optimized $LNP_{ssPalmE}$ composed of ssPalmE/SOPC/Chol (3/4/3) modified with DSG-PEG_{5000} were intravenously administered. At 48 h after transfection, the transgene expression was visualized by means of in vivo imaging with the IVIS Lumina II. The tumor tissues were depicted by red arrowhead.

The effect of the type of pDNA was also evaluated. The gene expression of $LNP_{ssPalmE}$ in tumor tissue was decreased by one order of magnitude when the pDNA was replaced from pCpGfree-Luc(0) to the conventionally used pDNA (pcDNA3.1-GL3) containing 332 CpG-motifs (**Supplemental Figure S1**). Thus, the use of pDNA that is free of the CpG-motif is also a key factor for the successful transgene expression in tumors, as has been demonstrated previously for the liver [33].

3.4. Antitumor effect of the delivery of pDNA encoding sFlt-1

Finally, the anti-tumor activity was evaluated by the repeated administration of LNP that encapsulated the pDNA encoding sFlt-1 (**Figure 5A**). As described above, the use of pDNA free from the CpG-motif is a key factor for the successful gene expression in tumors. Thus, all of the CpG motifs (76 CpG motifs) in sFlt-1 were replaced with other codons that are translated to the same amine (**Supplemental Figure S2**), and were then inserted into the pCpG-free vector to prepare the pCpGfree-sFlt-1(0).

In comparison with the PBS-injected group, the injection of the $LNP_{ssPalmM}$ or $LNP_{ssPalmE}$ encapsulating pCpGfree-sFlt-1(0) (closed triangle and circles, respectively) suppressed tumor growth, while the therapeutic effect of the corresponding particles encapsulating luciferase-encoding pDNA (pCpGfree-sFlt-1(0)) showed little or only marginal effects (open triangle and circles, respectively). It is noteworthy that the anti-tumor effect of $LNP_{ssPalmE}$ was significantly higher than that for $LNP_{ssPalmM}$. Throughout these experiments, no decrease in body weight was observed in any of the groups (**Figure 5B**).

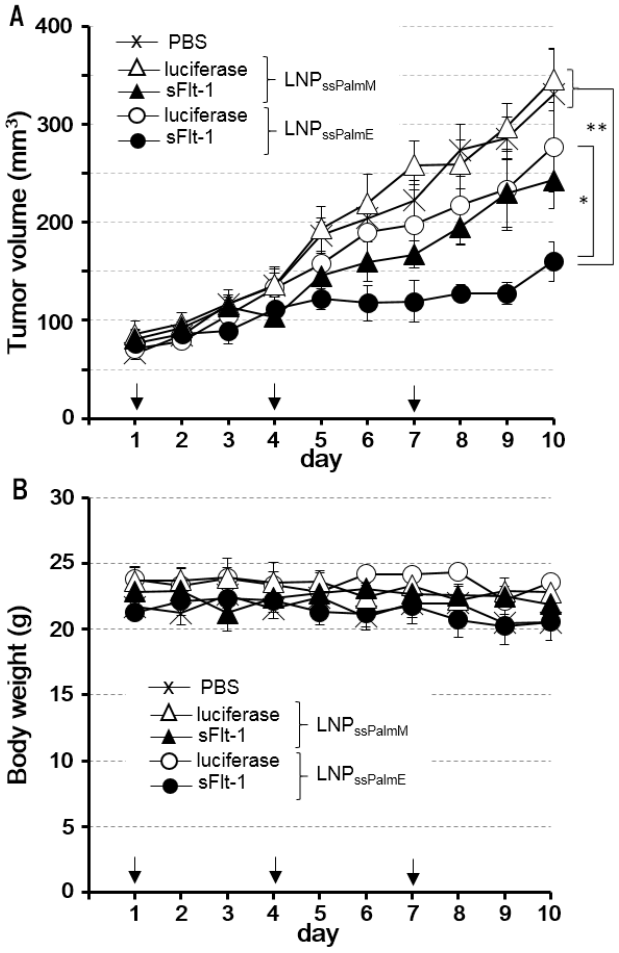

Fig.5 Comparison of the therapeutic effect of $LNP_{ssPalmM}$ and $LNP_{ssPalmE}$ encapsulating CpG-free pDNA encoding sFlt-1

$LNP_{ssPalmM}$ (triangles) or $LNP_{ssPalmE}$ (circles) encapsulating pCpGfree-Luc(0) (open) or pCpGfree-sFlt-1(0) (closed) were administered intravenously 3 times at every 3 days (arrowhead). The cross symbols represent the control groups in those PBS were administered. Tumor volume (A) and body weight (B) was monitored at the indicated times. Data are expressed as the mean ± S.E. (n=6). Statistical analyses were performed by One-way ANOVA followed by Bonferroni's multiple comparison test (*; $p<0.05$, **; $p<0.01$).

To gain more insight into the mechanism of the anti-tumor effect, sFlt-1 gene expression was confirmed by RT-PCR. As shown in **Figure 6A**, sFlt-1 gene expression was actually detected in all of the 3 mice that were analyzed, only when pDNA encoding sFlt-1 was delivered to the tumor. No band was detected when reverse transcription process was omitted. Thus, the band is derived from the cDNA that was reverse-transcribed from the mRNA, and not from the contaminating pDNA. Finally, the anti-angiogenic effect was confirmed by staining endothelial cells using FITC–GSI-B4. The quantified vascular density (**Figure 6B**) was significantly lower than that for the PBS-treated group when pDNA encoding sFlt-1 was delivered by $LNP_{ssPalmE}$ ($p < 0.05$), while it was not significant in mice treated with luciferase-encoding pDNA. Also, it is likely that the length of each vasculature was shorted when sFlt-1 gene was delivered (**Figure 6C**) in comparison with other control groups. Collectively, $LNP_{ssPalmE}$ encapsulating pGpGfree-sFlt-1(0) appears to be a promising and safe carrier for RCC-targeting gene delivery and tumor suppression by virtue of the obstruction of the tumor neovasculature.

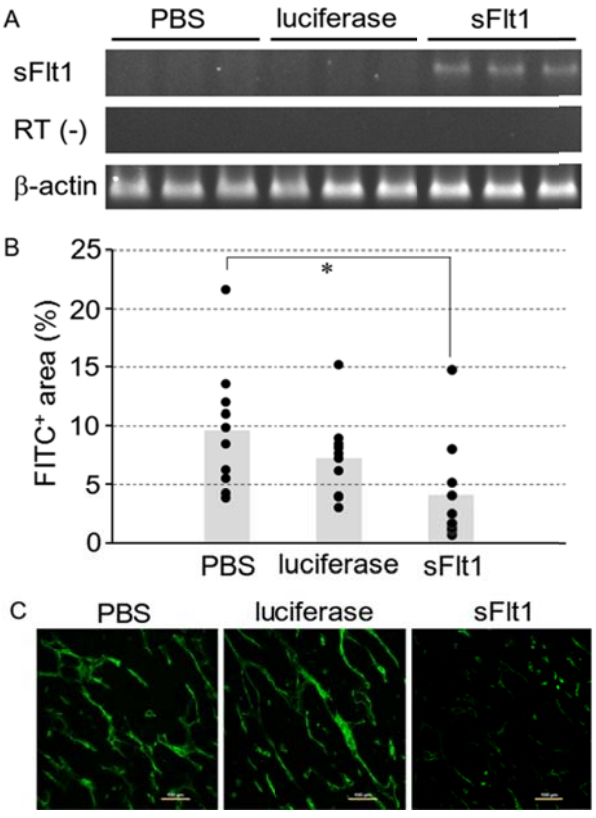

Fig.6. Anti-angiogenic effect by the delivery pDNA encoding sFlt-1 by LNPssPalmE.

(A) PBS and $LNP_{ssPalmE}$ encapsulating pCpGfree-Luc(0) or pCpGfree-sFlt-1(0) were administered intravenously in OSRC2-bearing mice. 48 h after the administration, tumor tissue was corrected. The mRNA expression of sFlt-1 (top) and β-actin as an internal control (bottom) in individual 3 mice was evaluated by RT-PCR, followed by gel electrophoresis. As an additional control, the PCR reaction was demonstrated without reverse transcription (middle). (B) PBS and $LNP_{ssPalmE}$ encapsulating pCpGfree-Luc(0) or pCpGfree-sFlt-1(0) were administered twice with 3-day interval. At 48 h after the second dose, the tumor vasculature was immune-stained with FITC–GSI-B4. The 10 confocal images were randomly captured in each group. The fraction of the FITC–GSI-B4-positive pixel area to the total pixels in total one was plotted. Bars represent a mean values. Statistical analyses were performed by Mann-Whitney test ($P < 0.05$). (C) Typical images of the tumor vasculature stained with FITC–GSI-B4 were shown. Bars: 100 μm.

4. Discussion

In the present study, we report on successful tumor-specific gene delivery by means of $LNP_{ssPalmE}$. Certain types of neutral liposomes [41] or siRNA-encapsulating lipid nanoparticle prepared with pH-sensitive lipids [42] were inherently and extensively taken up by the liver after the intravenous administration with the aid of apolipoprotein E (ApoE) that was bound on the particle surface. The ApoE-dependent acceleration of cellular uptake into mouse liver hepatoma cells (Hepa1c1c7 cells) was also confirmed in siRNA-encapsulating $LNP_{ssPalmE}$ (Noguchi *et al.*, unpublished observation). Also, undesired interactions with serum proteins (i.e. opsonins) can induce rapid clearance by the reticuloendothelial system (RES) [43, 44]. For successful tumor accumulation of a nanoparticle by the EPR effect, prolonged circulation in the blood is a crucial factor. To reduce the extent of interactions with blood components and immune responses, shielding the surface with the hydrophilic PEG polymer is the gold-standard strategy [44-46]. In the present study, we used two types of PEG-lipids in which myristoyl- or stearyl chains were used as a hydrophobic scaffold (DMG-PEG and DSG-PEG, respectively). 3 mol% of DMG-PEG_{2000} was incorporated in all LNP_{ssPalm} preparations to avoid the aggregation of neutralized particles at physiological pH, in that particle–to-particle electrostatic repulsion was poor. DMG-PEG_{2000} does not provide stability in blood circulation, but had a minimum effect on the intracellular trafficking processes [23, 47]. Thus, DSG-PEG_{2000} was additionally incorporated into the particle, to prolong its lifetime in the blood circulation [23, 31]. However, PEG modification adversely inhibits the cellular uptake of the endosomal escape process by preventing the interaction of the lipid envelope with biomembranes (i.e. plasma membrane or endosomes) [37, 47-51]. Thus, to overcome this “PEG dilemma”, it is necessary to determine the optimum density or length of the PEG in order to achieve optimal retention. We previously used a cationic lipid (N-[1-(2,3-Dioleoyloxy)propyl]-N,N,N-trimethylammonium: DOTAP) as a component of the lipid envelope for tumor targeting. In this case, 15 mol% PEG-lipid was necessary to aid in prolonging the lifetime of the particle in the circulation [37, 52]. In contrast, 5 mol% PEG-lipid is sufficient to confer a comparable or higher level of blood circulation in the case of the $LNP_{ssPalmM}$ (**Figure 1**). Thus, the use of a neutralized particle is advantageous in terms of overcoming the PEG dilemma issue. Meanwhile, the blood concentration of the $LNP_{ssPalmM}$ prepared with SOPE as a helper lipid was less than 3%ID/mL, and PEG-modification failed to

improve this. Liposomes composed of a helper lipid with phosphatidylethanolamine (PE) in the head group is inherently unstable in the blood in comparison to the groups on phosphatidylcholine (PC), presumably due to their fusogenic nature [53]. Moreover, liposomes containing PE activate the complement pathway and are closely related to the clearance of liposomes via macrophages [54]. Thus, a lipid containing PC in its head group is prerequisite as a helper lipid for successful tumor targeting of the LNP_{ssPalm}. Generally, the stability of a liposome in the blood circulation tends to increase, depending on the length and density of the PEG chains on the surface of the particle. However, the stability was not improved even when the density of PEG_{5000} was increased from 5 mol% to 10 mol%. In the present study, DSG-PEG_{2000} or DSG-PEG_{5000} was used to modify the LNPs after the preparation by a simple incubation with of PEG-lipids with the prepared particle. Thus, a surface coating with PEG_{5000} might be saturated at a level of 5 mol%.

In agreement with the above discussion, modification with PEG improved transgene expression in tumor tissue, accompanied by a decrease in hepatic gene expression (**Figure 3**). Of note, the transfection activities of $LNP_{ssPalmA}$ and $LNP_{ssPalmE}$ were decreased when the DSG-PEG_{5000} density was increased from 5 mol% to 10 mol%. Since the blood circulation property was comparable, regardless of the PEG density, it is plausible to assume that tumor accumulation would also be comparable in these groups. Thus, the inhibition of endosomal escape by extensive PEG-modification is the possible reason for the decrease in transgene expression.

Concerning the $LNP_{ssPalmA}$, we previously reported that the particles were actively transported to the nuclear periphery as intact particles, and consequently exhibited a 1 order of magnitude higher transfection activity than $LNP_{ssPalmM}$ *in vitro* HT1080 cells [34]. However, in the present study, the transfection activity in tumor tissue was comparable or somewhat less than that for the $LNP_{ssPalmM}$, whereas a comparable amount of pDNA was delivered (**Figure 2B**). In HT1080 cells, the nuclear transport and transgene expression of $LNP_{ssPalmA}$ was drastically prevented in the case of the exposure to an excess of retinoic acid. Thus, endogenous vitamin A-transporters such as cellular retinoic acid-binding proteins (CRABP) play a key role in the nuclear transport of $LNP_{ssPalmA}$. However, the expression level of CRABP I and II is down-regulated in RCC, while high levels of mRNA expression were found in normal kidney tissue [55, 56]. Thus, the CRABP-dependent transport machinery in the cytoplasm does not hold

promise in the nuclear delivery of $LNP_{ssPalmA}$ in RCC. Rather, the lower transgene expression in the case of $LNP_{ssPalmA}$ is due to the slower decapsulation of pDNA from the lipid envelope structure[34].

Finally, the $LNP_{ssPalmE}$ showed the strongest anti-tumor effect when it carried pDNA encoding sFlt-1 (**Figure 5**). The anti-tumor effect is highly dependent on whether or not sFlt-1 is encoded in the pDNA. Thus, preventing the development of the neovasculature is the most plausible mechanism for the observed tumor suppression. In fact, the density and length of the tumor vasculature was reduced in $LNP_{ssPalmE}$ when it carried the pDNA encoding sFlt-1 (**Figure 6B and 6C**). Thus, it is highly plausible that tumor cells might undergo apoptosis under the hypoxia environment due to the lack of angiogenesis and blood supply. The most significant finding is that the anti-tumor effect of $LNP_{ssPalmE}$ is measurably higher than $LNP_{ssPalmM}$, while $LNP_{ssPalmE}$ showed only a slightly higher transfection activity. This phenomena can be explained by assuming that the $LNP_{ssPalmE}$ itself has an anti-tumor effect. Hama *et al.* demonstrated that α-tocopherol succinate has apoptotic activity against cancer cells [57, 58], which is achieved by triggering the generation of nitric oxide and superoxide [59]. Thus, the α-tocopherol succinate generated by the degradation of ssPalmE might damage cancer cells. Therefore, the function of the sFlt-1 that is successfully expressed with an aid of $LNP_{ssPalmE}$ and the intrinsic function of α-tocopherol succinate as an inducer of apoptosis might synergistically function to achieve the extensive anti-tumor effect that was observed here.

5. Conclusion

The use of optimized PEG in preparing nanoparticles resulted in the tumor-specific gene expression in a solid RCC-bearing model. In addition, pDNA-encapsulating particles formed with ssPalmE showed strong anti-tumor effects due to the synergistic function of the gene product encoded in pDNA and $LNP_{ssPalmE}$. Collectively, the PEG-modified $LNP_{ssPalmE}$ is a promising gene carrier for targeting tumors for curing RCC with an aid of the therapeutic gene and the carrier *per se*.

Acknowledgement

This work was supported in part by Funding Program for Next Generation World-Leading Researchers (NEXT program; LR001). This investigation is also supported in part by The Mochida Memorial Foundation for Medical and Pharmaceutical Research, and The Asahi Glass Foundation. The authors would also like to thank Dr. M. S. Feather for his helpful advice in writing the English manuscript.

Figure Legends

Fig.1. Time profiles for the concentration of $LNP_{ssPalmM}$ in the blood.

The $LNP_{ssPalmM}$ modified with DSG-PEG_{2000} or DSG-PEG_{5000} at various density (5% or 10%) were labeled with [^{3}H]CHE, and then administered intravenously. The time profiles for the blood concentration were represented by %ID/mL. Circle and square symbols represent the $LNP_{ssPalmM}$ prepared with SOPE and SOPC as a helper lipid, respectively. Open and closed symbols represent the $LNP_{ssPalmM}$ modified with DSG-PEG_{2000} and unmodified one, respectively. The triangles represent the $LNP_{ssPalmM}$ prepared with SOPC that were modified with 5mol% (closed symbols) and 10 mol% (open symbols) of DSG-PEG_{5000}, respectively. Data were represented as the mean ± S.D. of triplicate experiments. Statistical analyses were performed by One-way ANOVA followed by Bonferroni's multiple comparison test (*; $p<0.05$, **; $p<0.01$).

Fig.2. Effect of the hydrophobic scaffold on the accumulation and stability of pDNA in tumor tissue

(A) Chemical structures of ssPalmM, ssPalmA and ssPalmE. Myristic acid, retinoic acid and α-tocopherol succinate were used as a hydrophobic scaffold. These materials mount ternary amines as a proton-sponge unit and disulfide bonding as a reductive environment-responsive cleavage unit. (B) Tumor samples were collected at 24 h (closed bars) and 48 hr (open bars) after the intravenous administration of $LNP_{ssPalmM}$, $LNP_{ssPalmA}$ and $LNP_{ssPalmE}$ for the separation of total DNA. The DNA samples were subjected to real-time PCR for the quantification of copy numbers of pDNA in tumor. Data are expressed as the mean ± S.D. of triplicate experiments. Statistical analyses were performed by One-way ANOVA followed by Student-Newman-Keuls test (*; $p<0.05$, **; $p<0.01$).

Fig.3. *in vivo* transgene expression in tumors

LNP was prepared using various combinations of ssPalms (ssPalmM, ssPalmA and ssPalmE), helper lipids (SOPE and SOPC) and PEG lipids (DSG-PEG_{2000} and DSG-PEG_{5000}). Transfection activities were evaluated at 48 h after the intravenous administration of the particles at a dose of 40 μg/mouse. Statistical analyses were performed by One-way ANOVA followed by Newman-Keuls multiple comparison test (*; $p<0.05$, **; $p<0.01$).

Fig.4. Optical images of the *in vivo* transgene expression

Optimized $LNP_{ssPalmE}$ composed of ssPalmE/SOPC/Chol (3/4/3) modified with DSG-PEG_{5000} were intravenously administered. At 48 h after transfection, the transgene expression was visualized by means of *in vivo* imaging with the IVIS Lumina II. The tumor tissues were depicted by red arrowhead.

Fig.5. Comparison of the therapeutic effect of $LNP_{ssPalmM}$ and $LNP_{ssPalmE}$ encapsulating CpG-free pDNA encoding sFlt-1.

$LNP_{ssPalmM}$ (triangles) or $LNP_{ssPalmE}$ (circles) encapsulating pCpGfree-Luc(0) (open) or pCpGfree-sFlt-1(0) (closed) were administered intravenously 3 times at every 3 days (arrowhead). The cross symbols represent the control groups in those PBS were administered. Tumor volume (A) and body weight (B) was monitored at the indicated times. Data are expressed as the mean ± S.E. (n=6). Statistical analyses were performed by One-way ANOVA followed by Bonferroni's multiple comparison test (*; $p<0.05$, **; $p<0.01$) .

Fig.6. Anti-angiogenic effect by the delivery pDNA encoding sFlt-1 by $LNP_{ssPalmE}$.

(A) PBS and $LNP_{ssPalmE}$ encapsulating pCpGfree-Luc(0) or pCpGfree-sFlt-1(0) were administered intravenously to OSRC2-bearing mice. At 48 h after the administration, tumor tissue was collected. mRNA expression of sFlt-1 (top) and β-actin as an internal control (bottom) in individual 3 mice was evaluated by RT-PCR, followed by gel electrophoresis. As an additional control, the PCR reaction was carried out without reverse transcription (middle). (B) PBS and $LNP_{ssPalmE}$ encapsulating pCpGfree-Luc(0) or pCpGfree-sFlt-1(0) were administered twice at 3-day intervals. At 48 h after the second dose, the tumor vasculature was immune-

stained with FITC–GSI-B4. The 10 confocal images were randomly captured in each group. The fraction of the FITC–GSI-B4-positive pixel area to the total pixels in total one was plotted. Bars represent mean values. Statistical analyses were performed One-way ANOVA followed by SNK test ($P < 0.05$). (C) Typical images of the tumor vasculature stained with FITC–GSI-B4 were shown. Bars: 100 μm.

References

[1] T. Wirth, N. Parker, S. Yla-Herttuala, History of gene therapy, Gene, 525 (2013) 162-169.

[2] A. Flemming, Regulatory watch: pioneering gene therapy on brink of approval, Nat Rev Drug Discov, 11 (2012) 664.

[3] D. Melchiorri, L. Pani, P. Gasparini, G. Cossu, J. Ancans, J.J. Borg, C. Drai, P. Fiedor, E. Flory, I. Hudson, H.G. Leufkens, J. Muller-Berghaus, G. Narayanan, B. Neugebauer, J. Pokrotnieks, J.L. Robert, T. Salmonson, C.K. Schneider, Regulatory evaluation of Glybera in Europe - two committees, one mission, Nat Rev Drug Discov, 12 (2013) 719.

[4] W.H. Chow, S.S. Devesa, J.L. Warren, J.F. Fraumeni, Jr., Rising incidence of renal cell cancer in the United States, JAMA, 281 (1999) 1628-1631.

[5] W.H. Chow, L.M. Dong, S.S. Devesa, Epidemiology and risk factors for kidney cancer, Nat Rev Urol, 7 (2010) 245-257.

[6] J. Li, H.K. Weir, M.A. Jim, S.M. King, R. Wilson, V.A. Master, Kidney Cancer Incidence and Mortality Among American Indians and Alaska Natives in the United States, 1990-2009, Am J Public Health, (2014).

[7] N.J. Vogelzang, W.M. Stadler, Kidney cancer, Lancet, 352 (1998) 1691-1696.

[8] G. Kibria, H. Hatakeyama, N. Ohga, K. Hida, H. Harashima, The effect of liposomal size on the targeted delivery of doxorubicin to Integrin alphavbeta3-expressing tumor endothelial cells, Biomaterials, 34 (2013) 5617-5627.

[9] E. Soto-Vega, C. Arroyo, Y. Richaud-Patin, M. Garcia-Carrasco, L.G. Vazquez-Lavista, L. Llorente, P-glycoprotein activity in renal clear cell carcinoma, Urol Oncol, 27 (2009) 363-366.

[10] T. Janowitz, S.J. Welsh, K. Zaki, P. Mulders, T. Eisen, Adjuvant therapy in renal cell carcinoma-past, present, and future, Semin Oncol, 40 (2013) 482-491.

[11] D.F. McDermott, M.B. Atkins, Immune therapy for kidney cancer: a second dawn?, Semin Oncol, 40 (2013) 492-498.

[12] A.M. Molina, R.J. Motzer, D.Y. Heng, Systemic treatment options for untreated patients with metastatic clear cell renal cancer, Semin Oncol, 40 (2013) 436-443.

[13] L.M. Randall, B.J. Monk, Bevacizumab toxicities and their management in ovarian cancer, Gynecol Oncol, 117 (2010) 497-504.

[14] S.L. Ginn, I.E. Alexander, M.L. Edelstein, M.R. Abedi, J. Wixon, Gene therapy clinical trials worldwide to 2012 - an update, J Gene Med, 15 (2013) 65-77.

[15] P.L. Felgner, T.R. Gadek, M. Holm, R. Roman, H.W. Chan, M. Wenz, J.P. Northrop, G.M. Ringold, M. Danielsen, Lipofection: a highly efficient, lipid-mediated DNA-transfection procedure, Proc Natl Acad Sci U S A, 84 (1987) 7413-7417.

[16] K.A. Mislick, J.D. Baldeschwieler, Evidence for the role of proteoglycans in cation-mediated gene transfer, Proc Natl Acad Sci U S A, 93 (1996) 12349-12354.

[17] C.M. Varga, N.C. Tedford, M. Thomas, A.M. Klibanov, L.G. Griffith, D.A. Lauffenburger, Quantitative comparison of polyethylenimine formulations and adenoviral vectors in terms of intracellular gene delivery processes, Gene Ther, 12 (2005) 1023-1032.

[18] S. Hama, H. Akita, S. Iida, H. Mizuguchi, H. Harashima, Quantitative and mechanism-based investigation of post-nuclear delivery events between adenovirus and lipoplex, Nucleic Acids Res, 35 (2007) 1533-1543.

[19] S. Hama, H. Akita, R. Ito, H. Mizuguchi, T. Hayakawa, H. Harashima, Quantitative comparison of intracellular trafficking and nuclear transcription between adenoviral and lipoplex systems, Mol Ther, 13 (2006) 786-794.

[20] R. Kircheis, L. Wightman, A. Schreiber, B. Robitza, V. Rossler, M. Kursa, E. Wagner, Polyethylenimine/DNA complexes shielded by transferrin target gene expression to tumors after systemic application, Gene Ther, 8 (2001) 28-40.

[21] F. Sakurai, T. Nishioka, F. Yamashita, Y. Takakura, M. Hashida, Effects of erythrocytes and serum proteins on lung accumulation of lipoplexes containing cholesterol or DOPE as a helper lipid in the single-pass rat lung perfusion system, Eur J Pharm Biopharm, 52 (2001) 165-172.

[22] T. Nomoto, Y. Matsumoto, K. Miyata, M. Oba, S. Fukushima, N. Nishiyama, T. Yamasoba, K. Kataoka, In situ quantitative monitoring of polyplexes and polyplex micelles in the blood circulation using intravital real-time confocal laser scanning microscopy, J Control Release, 151 (2011) 104-109.

[23] E. Ambegia, S. Ansell, P. Cullis, J. Heyes, L. Palmer, I. MacLachlan, Stabilized plasmid-lipid particles containing PEG-diacylglycerols exhibit extended circulation lifetimes and tumor selective gene expression, Biochim Biophys Acta, 1669 (2005) 155-163.

[24] L.B. Jeffs, L.R. Palmer, E.G. Ambegia, C. Giesbrecht, S. Ewanick, I. MacLachlan, A scalable, extrusion-free method for efficient liposomal encapsulation of plasmid DNA, Pharm Res, 22 (2005) 362-372.

[25] P. Tam, M. Monck, D. Lee, O. Ludkovski, E.C. Leng, K. Clow, H. Stark, P. Scherrer, R.W. Graham, P.R. Cullis, Stabilized plasmid-lipid particles for systemic gene therapy, Gene Ther, 7 (2000) 1867-1874.

[26] J. Heyes, L. Palmer, K. Chan, C. Giesbrecht, L. Jeffs, I. MacLachlan, Lipid encapsulation enables the effective systemic delivery of polyplex plasmid DNA, Mol Ther, 15 (2007) 713-720.

[27] M. Jayaraman, S.M. Ansell, B.L. Mui, Y.K. Tam, J. Chen, X. Du, D. Butler, L. Eltepu, S. Matsuda, J.K. Narayanannair, K.G. Rajeev, I.M. Hafez, A. Akinc, M.A. Maier, M.A. Tracy, P.R. Cullis, T.D. Madden, M. Manoharan, M.J. Hope, Maximizing the potency of siRNA lipid nanoparticles for hepatic gene silencing in vivo, Angew Chem Int Ed Engl, 51 (2012) 8529-8533.

[28] A.D. Judge, V. Sood, J.R. Shaw, D. Fang, K. McClintock, I. MacLachlan, Sequence-dependent stimulation of the mammalian innate immune response by synthetic siRNA, Nat Biotechnol, 23 (2005) 457-462.

[29] M.A. Maier, M. Jayaraman, S. Matsuda, J. Liu, S. Barros, W. Querbes, Y.K. Tam, S.M. Ansell, V. Kumar, J. Qin, X. Zhang, Q. Wang, S. Panesar, R. Hutabarat, M. Carioto, J. Hettinger, P. Kandasamy, D. Butler, K.G. Rajeev, B. Pang, K. Charisse, K. Fitzgerald, B.L. Mui, X. Du, P. Cullis, T.D. Madden, M.J. Hope, M. Manoharan, A. Akinc, Biodegradable lipids enabling rapidly eliminated lipid nanoparticles for systemic delivery of RNAi therapeutics, Mol Ther, 21 (2013) 1570-1578.

[30] Y. Sakurai, H. Hatakeyama, Y. Sato, H. Akita, K. Takayama, S. Kobayashi, S. Futaki, H. Harashima, Endosomal escape and the knockdown efficiency of liposomal-siRNA by the fusogenic peptide shGALA, Biomaterials, 32 (2011) 5733-5742.

[31] Y. Sakurai, H. Hatakeyama, Y. Sato, M. Hyodo, H. Akita, H. Harashima, Gene silencing via RNAi and siRNA quantification in tumor tissue using MEND, a liposomal siRNA delivery system, Mol Ther, 21 (2013) 1195-1203.

[32] H. Akita, R. Ishiba, H. Hatakeyama, H. Tanaka, Y. Sato, K. Tange, M. Arai, K. Kubo, H. Harashima, A Neutral Envelope-Type Nanoparticle Containing pH-Responsive and SS-Cleavable Lipid-Like Material as a Carrier for Plasmid DNA, Adv Healthc Mater, 2 (2013) 1120-1125.
[33] M. Ukawa, H. Akita, Y. Hayashi, R. Ishiba, K. Tange, M. Arai, K. Kubo, Y. Higuchi, K. Shimizu, S. Konishi, M. Hashida, H. Harashima, Neutralized Nanoparticle Composed of SS-Cleavable and pH-Activated Lipid-Like Material as a Long-Lasting and Liver-Specific Gene Delivery System, Adv Healthc Mater, (in press).
[34] H. Tanaka, H. Akita, R. Ishiba, K. Tange, M. Arai, K. Kubo, H. Harashima, Neutral biodegradable lipid-envelope-type nanoparticle using vitamin A-Scaffold for nuclear targeting of plasmid DNA, Biomaterials, 35 (2014) 1755-1761.
[35] M. Shibuya, Vascular endothelial growth factor and its receptor system: physiological functions in angiogenesis and pathological roles in various diseases, J Biochem, 153 (2013) 13-19.
[36] H. Akita, S. Ishii, N. Miura, S.M. Shaheen, Y. Hayashi, T. Nakamura, N. Kaji, Y. Baba, H. Harashima, A DNA microarray-based analysis of immune-stimulatory and transcriptional responses of dendritic cells to KALA-modified nanoparticles, Biomaterials, 34 (2013) 8979-8990.
[37] H. Hatakeyama, H. Akita, K. Kogure, M. Oishi, Y. Nagasaki, Y. Kihira, M. Ueno, H. Kobayashi, H. Kikuchi, H. Harashima, Development of a novel systemic gene delivery system for cancer therapy with a tumor-specific cleavable PEG-lipid, Gene Ther, 14 (2007) 68-77.
[38] H. Hatakeyama, H. Akita, K. Maruyama, T. Suhara, H. Harashima, Factors governing the in vivo tissue uptake of transferrin-coupled polyethylene glycol liposomes in vivo, Int J Pharm, 281 (2004) 25-33.
[39] D. Peer, J.M. Karp, S. Hong, O.C. Farokhzad, R. Margalit, R. Langer, Nanocarriers as an emerging platform for cancer therapy, Nat Nanotechnol, 2 (2007) 751-760.
[40] S.C. Hyde, I.A. Pringle, S. Abdullah, A.E. Lawton, L.A. Davies, A. Varathalingam, G. Nunez-Alonso, A.M. Green, R.P. Bazzani, S.G. Sumner-Jones, M. Chan, H. Li, N.S. Yew, S.H. Cheng, A.C. Boyd, J.C. Davies, U. Griesenbach, D.J. Porteous, D.N. Sheppard, F.M. Munkonge, E.W. Alton, D.R. Gill, CpG-free plasmids confer reduced inflammation and sustained pulmonary gene expression, Nat Biotechnol, 26 (2008) 549-551.
[41] X. Yan, F. Kuipers, L.M. Havekes, R. Havinga, B. Dontje, K. Poelstra, G.L. Scherphof, J.A. Kamps, The role of apolipoprotein E in the elimination of liposomes from blood by hepatocytes in the mouse, Biochem Biophys Res Commun, 328 (2005) 57-62.
[42] A. Akinc, W. Querbes, S. De, J. Qin, M. Frank-Kamenetsky, K.N. Jayaprakash, M. Jayaraman, K.G. Rajeev, W.L. Cantley, J.R. Dorkin, J.S. Butler, L. Qin, T. Racie, A. Sprague, E. Fava, A. Zeigerer, M.J. Hope, M. Zerial, D.W. Sah, K. Fitzgerald, M.A. Tracy, M. Manoharan, V. Koteliansky, A. Fougerolles, M.A. Maier, Targeted delivery of RNAi therapeutics with endogenous and exogenous ligand-based mechanisms, Mol Ther, 18 (2010) 1357-1364.
[43] T. Ishida, H. Harashima, H. Kiwada, Liposome clearance, Biosci Rep, 22 (2002) 197-224.
[44] M. Ogris, S. Brunner, S. Schuller, R. Kircheis, E. Wagner, PEGylated DNA/transferrin-PEI complexes: reduced interaction with blood components, extended circulation in blood and potential for systemic gene delivery, Gene Ther, 6 (1999) 595-605.
[45] H. Hatakeyama, E. Ito, M. Yamamoto, H. Akita, Y. Hayashi, K. Kajimoto, N. Kaji, Y. Baba, H. Harashima, A DNA microarray-based analysis of the host response to a nonviral gene carrier: a strategy for improving the immune response, Mol Ther, 19 (2011) 1487-1498.
[46] A. Koshkaryev, R. Sawant, M. Deshpande, V. Torchilin, Immunoconjugates and long circulating systems: origins, current state of the art and future directions, Adv Drug Deliv Rev, 65 (2013) 24-35.
[47] Y. Sato, H. Hatakeyama, Y. Sakurai, M. Hyodo, H. Akita, H. Harashima, A pH-sensitive cationic lipid facilitates the delivery of liposomal siRNA and gene silencing activity in vitro and in vivo, J Control Release, 163 (2012) 267-276.

[48] H. Hatakeyama, H. Akita, H. Harashima, A multifunctional envelope type nano device (MEND) for gene delivery to tumours based on the EPR effect: a strategy for overcoming the PEG dilemma, Adv Drug Deliv Rev, 63 (2011) 152-160.
[49] H. Hatakeyama, H. Akita, H. Harashima, The polyethyleneglycol dilemma: advantage and disadvantage of PEGylation of liposomes for systemic genes and nucleic acids delivery to tumors, Biol Pharm Bull, 36 (2013) 892-899.
[50] S. Mishra, P. Webster, M.E. Davis, PEGylation significantly affects cellular uptake and intracellular trafficking of non-viral gene delivery particles, Eur J Cell Biol, 83 (2004) 97-111.
[51] K. Remaut, B. Lucas, K. Braeckmans, J. Demeester, S.C. De Smedt, Pegylation of liposomes favours the endosomal degradation of the delivered phosphodiester oligonucleotides, J Control Release, 117 (2007) 256-266.
[52] H. Hatakeyama, H. Akita, E. Ito, Y. Hayashi, M. Oishi, Y. Nagasaki, R. Danev, K. Nagayama, N. Kaji, H. Kikuchi, Y. Baba, H. Harashima, Systemic delivery of siRNA to tumors using a lipid nanoparticle containing a tumor-specific cleavable PEG-lipid, Biomaterials, 32 (2011) 4306-4316.
[53] M.C. De Oliveira, V. Boutet, E. Fattal, D. Boquet, J.M. Grognet, P. Couvreur, J.R. Deverre, Improvement of in vivo stability of phosphodiester oligonucleotide using anionic liposomes in mice, Life Sci, 67 (2000) 1625-1637.
[54] C. Mold, Effect of membrane phospholipids on activation of the alternative complement pathway, J Immunol, 143 (1989) 1663-1668.
[55] U. Goelden, S. Pfoertner, W. Hansen, T. Toepfer, R. von Knobloch, R. Hofmann, J. Buer, A.J. Schrader, Expression and functional influence of cellular retinoic acid-binding protein II in renal cell carcinoma, Urol Int, 75 (2005) 269-276.
[56] S. Pfoertner, U. Goelden, W. Hansen, T. Toepfer, R. Geffers, S.N. Ukena, R. von Knobloch, R. Hofmann, J. Buer, A.J. Schrader, Cellular retinoic acid binding protein I: expression and functional influence in renal cell carcinoma, Tumour Biol, 26 (2005) 313-323.
[57] S. Hama, K. Kogure, Nanoparticles consisting of tocopheryl succinate are a novel drug-delivery system with multifaceted antitumor activity, Biol Pharm Bull, 37 (2014) 196-200.
[58] S. Hama, S. Utsumi, Y. Fukuda, K. Nakayama, Y. Okamura, H. Tsuchiya, K. Fukuzawa, H. Harashima, K. Kogure, Development of a novel drug delivery system consisting of an antitumor agent tocopheryl succinate, J Control Release, 161 (2012) 843-851.
[59] K. Fukuzawa, K. Kogure, M. Morita, S. Hama, S. Manabe, A. Tokumura, Enhancement of nitric oxide and superoxide generations by alpha-tocopheryl succinate and its apoptotic and anticancer effects, Biochemistry (Mosc), 69 (2004) 50-57.